

1 Electronic Supporting Information

2 Effect of Secondary Organic Aerosol from Isoprene-Derived Hydroxyhydroperoxides on 3 the Expression of Oxidative Stress Response Genes in Human Bronchial Epithelial Cells

5 Maiko Arashiro^{1,a}, Ying-Hsuan Lin^{1,b}, Zhenfa Zhang¹, Kenneth G. Sexton¹, Avram Gold¹, Ilona
6 Jaspers^{1,2}, Rebecca C. Fry¹, Jason D. Surratt^{1,*}

7 ¹Department of Environmental Sciences and Engineering, Gillings School of Global Public
8 Health, The University of North Carolina at Chapel Hill, Chapel Hill, North Carolina, USA

9 ²Department of Pediatrics, School of Medicine, The University of North Carolina at Chapel Hill,
10 Chapel Hill, North Carolina, USA

11 ^aCurrent address: Department of Environmental Studies, Dickinson College, Carlisle,
12 Pennsylvania 17013, USA

13 ^bCurrent address: Department of Environmental Sciences, Environmental Toxicology Graduate
14 Program, University of California, Riverside, California 92521, USA

15
16 *To whom correspondence should be addressed.

17 Tel: (919)-966-0470. Fax: (919)-966-7911. Email: surratt@unc.edu (J.D.S.)

20 *Generation and Chemical Characterization of Isoprene-Derived SOA and ISOPOOH-Derived* 21 *SOA*

22 Isoprene-derived SOA used for cellular exposure were generated by photochemically
23 oxidizing a mixture of acidified sulfate seed aerosol, isoprene, and NO injected into an outdoor
24 smog chamber facility. The generation and chemical characterization of the isoprene-derived
25 SOA used for the resuspension exposures in this study has been described in detail as part of a
26 previous study.¹

27 ISOPOOH-derived SOA were generated in a 10-m³ flexible Teflon indoor chamber at the
28 University of North Carolina, as recently described by Riva et al.² Experiments were performed
29 at room temperature (25°C) under dark and low relative humidity (RH) (<5%) conditions. Prior
30 to each experiment, the chamber was flushed for at least 24 hrs to replace at least five volumes of
31 chamber air to ensure particle-free conditions and O₃ and VOC concentrations were below
32 detection limits. Aerosol size distributions were measured continuously using a differential

33 mobility analyzer (DMA; BMI model 2002) coupled to a mixing condensation particle counter
34 (MCPC; BMI model 1710). The O_3 concentration was monitored over the course of the
35 experiment using a UV photometric analyzer (Model 49P, Thermo-Environmental). Temperature
36 and RH inside the chamber were continuously monitored using an OM-62 temperature RH data
37 logger (OMEGA Engineering, Inc.).

38 A neutral ammonium sulfate $((NH_4)_2SO_4)$ seed aerosol solution containing 0.06 M
39 $(NH_4)_2SO_4$ was atomized into the chamber until the total aerosol mass concentration in the
40 chamber was $\sim 80 \mu g m^{-3}$. Because 90% of ISOPOOH + OH yields IEPOX, neutral $(NH_4)_2SO_4$
41 seed was used to prevent the reactive uptake of IEPOX and allow the 10% of hydroperoxides to
42 condense onto pre-existing aerosol.³ Following aerosol injection, 300 ppb of 1,2-ISOPOOH,
43 synthesized in house as described by Riva et al.,² was injected into the chamber by passing high-
44 purity N_2 gas through a manifold heated to $\sim 70^\circ C$ at $2 L min^{-1}$ for 10 mins then at $5 L min^{-1}$ for
45 80 mins. O_3 was introduced into the chamber using an O_3 generator (model L21, Pacific ozone)
46 followed by a continuous injection of tetramethylethylene (TME). The ozonolysis of TME
47 formed the OH radicals needed for the oxidation of ISOPOOH. A summary of the experimental
48 conditions is given in Table S1. Neutral $(NH_4)_2SO_4$ seed aerosol only experiments served as
49 controls. Following the 1.5-hr injection of TME, aerosol samples were collected onto Teflon
50 membrane filters (47 mm diameter, $1.0 \mu m$ pore size; Pall Life Science). Exact mass loadings on
51 the filters were calculated from total air volume sampled and average mass concentrations of
52 aerosol during the sampling period. A density correction of $1.6 g cm^{-3}$ ⁴ and $1.25 g cm^{-3}$ ⁵ was
53 applied to convert the measured volume concentrations to mass concentrations for the $(NH_4)_2SO_4$
54 seed and SOA growth.

55 **DTT methods**

56 Description of the DTT assay has been previously described in detail.⁶⁻⁷ Briefly, DTT
57 and DTNB stock solutions were made by adding DTT standard (powder form) (Sigma-Aldrich)
58 or DTNB standard (Sigma-Aldrich) to an aqueous buffer solution containing 0.05 mol L⁻¹
59 potassium phosphate monobasic-sodium hydroxide (KH₂PO₄, pH 7.4, Fisher Scientific) and 1
60 mM ethylenediaminetetraacetic acid (EDTA, Sigma Aldrich). A stock solution of 1,4-
61 naphthoquinone (1,4-NQ) was made by dissolving 0.5 mg of 1,4-NQ in 0.5 mL dimethyl
62 sulfoxide (DMSO). Volumes of stock solutions were added to additional aqueous buffer to make
63 working solutions.

64 ISOPOOH-derived SOA extracts were prepared by sonicating chamber filters in high-
65 purity methanol (LC/MS CHROMASOLV, Sigma-Aldrich). Three separate filters were used
66 (n=3) and extracts were concentrated by drying under a gentle stream of nitrogen. Each
67 ISOPOOH-derived SOA extract was combined with buffer and 0.05 mM DTT working solution
68 and incubated at 37°C for 30 min. Reactions were quenched with the addition of a 1 mM DTNB
69 working solution. A DTT calibration curve was generated by varying DTT volumes with buffer
70 solution. A calibration curve of 1,4-NQ was generated by varying volumes of 1,4-NQ with a set
71 amount of DTT. The consumption of DTT was measured by the absorbance of 5-thio-2-
72 nitrobenzoic acid (TNB), formed by the oxidation of residual DTT with DTNB, at 412 nm using
73 a UV–Visible Spectrophotometer (Hitachi U-3300 dual beam spectrophotometer)⁷⁻⁸. Dilution
74 effects were taken into account by correcting the absorbance measurements for sample volume.

75 ROS generation potential was expressed as DTT activity (nmol of DTT
76 consumed/min/μg sample) and the normalized index of oxidant generation (NIOG) for
77 comparison with previously published studies⁷. As demonstrated by Rattanavaraha et al.⁷, an
78 index of oxidant generation (IOG) was calculated according to the following equation⁷:

$$IOG = \frac{Abs_0 - Abs'}{Abs_0} \times \frac{100}{T \times M}$$

where T is reaction time (min), M is sample mass (μg), Abs_0 and Abs' are initial absorbance and absorbance at time T, respectively. The NIOG calculation normalizes activity with respect to a 1,4-NQ standard as follows:

$$NIOG_{sample} = \frac{IOG_{sample}}{IOG_{1,4-NQ}}$$

Table S1. Summary of experimental condition for ISOPOOH oxidation experiments and control experiments.

Experiment	Precursor Concentration (ppb)	Target O_3 (ppm)	TME	Initial Seed ($\mu\text{g m}^{-3}$)	SOA Growth ($\mu\text{g m}^{-3}$)	sampling volume (m^3)	mass collected (μg)
ISOPOOH	300	1.5	yes	76.45	47.76	2.80	133.71
ISOPOOH	300	1.5	yes	76.99	52.44	2.66	139.76
ISOPOOH	300	1.5	yes	77.28	54.34	3.04	165.47
Seed only	-	-	no	587.54	-	0.45	267

Table S2. Gene symbols and full names of 84 oxidative stress-associated genes and housekeeping genes included in RT² Profiler™ PCR Array Human Oxidative Stress Pathway Plus (PAHS-065Y).

#	Gene Symbol	Full Name
1	<i>ALB</i>	Albumin
2	<i>ALOX12</i>	Arachidonate 12-lipoxygenase
3	<i>AOX1</i>	Aldehyde oxidase 1
4	<i>APOE</i>	Apolipoprotein E
5	<i>ATOX1</i>	ATX1 antioxidant protein 1 homolog (yeast)
6	<i>BNIP3</i>	BCL2/adenovirus E1B 19kDa interacting protein 3
7	<i>CAT</i>	Catalase
8	<i>CCL5</i>	Chemokine (C-C motif) ligand 5
9	<i>CCS</i>	Copper chaperone for superoxide dismutase
10	<i>CYBB</i>	Cytochrome b-245, beta polypeptide
11	<i>CYGB</i>	Cytoglobin
12	<i>DHCR24</i>	24-dehydrocholesterol reductase
13	<i>DUOX1</i>	Dual oxidase 1
14	<i>DUOX2</i>	Dual oxidase 2

15	<i>DUSP1</i>	Dual specificity phosphatase 1
16	<i>EPHX2</i>	Epoxide hydrolase 2, cytoplasmic
17	<i>EPX</i>	Eosinophil peroxidase
18	<i>FOXM1</i>	Forkhead box M1
19	<i>FTH1</i>	Ferritin, heavy polypeptide 1
20	<i>GCLC</i>	Glutamate-cysteine ligase, catalytic subunit
21	<i>GPX1</i>	Glutathione peroxidase 1
22	<i>GPX2</i>	Glutathione peroxidase 2 (gastrointestinal)
23	<i>GPX3</i>	Glutathione peroxidase 3 (plasma)
24	<i>GPX4</i>	Glutathione peroxidase 4 (phospholipid hydroperoxidase)
25	<i>GPX5</i>	Glutathione peroxidase 5 (epididymal androgen-related protein)
26	<i>GSR</i>	Glutathione reductase
27	<i>GSS</i>	Glutathione synthetase
28	<i>GSTP1</i>	Glutathione S-transferase pi 1
29	<i>GSTZ1</i>	Glutathione transferase zeta 1
30	<i>HSPA1A</i>	Heat shock 70kDa protein 1A
31	<i>KRT1</i>	Keratin 1
32	<i>LPO</i>	Lactoperoxidase
33	<i>MB</i>	Myoglobin
34	<i>MBL2</i>	Mannose-binding lectin (protein C) 2, soluble
35	<i>MPO</i>	Myeloperoxidase
36	<i>MPV17</i>	MpV17 mitochondrial inner membrane protein
37	<i>MSRA</i>	Methionine sulfoxide reductase A
38	<i>MT3</i>	Metallothionein 3
39	<i>NCF1</i>	Neutrophil cytosolic factor 1
40	<i>NCF2</i>	Neutrophil cytosolic factor 2
41	<i>NOS2</i>	Nitric oxide synthase 2, inducible
42	<i>NOX4</i>	NADPH oxidase 4
43	<i>NOX5</i>	NADPH oxidase, EF-hand calcium binding domain 5
44	<i>NUDT1</i>	Nudix (nucleoside diphosphate linked moiety X)-type motif 1
45	<i>PDLIM1</i>	PDZ and LIM domain 1
46	<i>PRDX1</i>	Peroxiredoxin 1
47	<i>PRDX2</i>	Peroxiredoxin 2
48	<i>PRDX3</i>	Peroxiredoxin 3
49	<i>PRDX4</i>	Peroxiredoxin 4
50	<i>PRDX5</i>	Peroxiredoxin 5
51	<i>PRDX6</i>	Peroxiredoxin 6
52	<i>PRNP</i>	Prion protein
53	<i>PTGS1</i>	Prostaglandin-endoperoxide synthase 1 (prostaglandin G/H synthase and cyclooxygenase)
54	<i>PTGS2</i>	Prostaglandin-endoperoxide synthase 2 (prostaglandin G/H synthase and cyclooxygenase)
55	<i>RNF7</i>	Ring finger protein 7
56	<i>VIMP</i>	Selenoprotein S

57	<i>SEPP1</i>	Selenoprotein P, plasma, 1
58	<i>SFTPD</i>	Surfactant protein D
59	<i>SIRT2</i>	Sirtuin 2
60	<i>SOD1</i>	Superoxide dismutase 1, soluble
61	<i>SOD2</i>	Superoxide dismutase 2, mitochondrial
62	<i>SOD3</i>	Superoxide dismutase 3, extracellular
63	<i>SQSTM1</i>	Sequestosome 1
64	<i>SRXN1</i>	Sulfiredoxin 1
65	<i>TPO</i>	Thyroid peroxidase
66	<i>TTN</i>	Titin
67	<i>TXNRD2</i>	Thioredoxin reductase 2
68	<i>UCP2</i>	Uncoupling protein 2 (mitochondrial, proton carrier)
69	<i>AKR1C2</i>	Aldo-keto reductase family 1, member C2 (dihydrodiol dehydrogenase 2; bile acid binding protein; 3-alpha hydroxysteroid dehydrogenase, type III)
70	<i>BAG2</i>	BCL2-associated athanogene 2
71	<i>FHL2</i>	Four and a half LIM domains 2
72	<i>GCLM</i>	Glutamate-cysteine ligase, modifier subunit
73	<i>GLA</i>	Galactosidase, alpha
74	<i>HMOX1</i>	Heme oxygenase (decycling) 1
75	<i>HSP90AA1</i>	Heat shock protein 90kDa alpha (cytosolic), class A member 1
76	<i>LHPP</i>	Phospholysine phosphohistidine inorganic pyrophosphate phosphatase
77	<i>NCOA7</i>	Nuclear receptor coactivator 7
78	<i>NQO1</i>	NAD(P)H dehydrogenase, quinone 1
79	<i>PTGR1</i>	Prostaglandin reductase 1
80	<i>SLC7A11</i>	Solute carrier family 7 (anionic amino acid transporter light chain, xc- system), member 11
81	<i>SPINK1</i>	Serine peptidase inhibitor, Kazal type 1
82	<i>TRAPPC6A</i>	Trafficking protein particle complex 6A
83	<i>TXN</i>	Thioredoxin
84	<i>TXNRD1</i>	Thioredoxin reductase 1
Housekeeping Genes	<i>ACTB</i>	Actin, beta
	<i>B2M</i>	Beta-2-microglobulin
	<i>GAPDH</i>	Glyceraldehyde-3-phosphate dehydrogenase
	<i>HPRT1</i>	Hypoxanthine phosphoribosyltransferase 1
	<i>RPLP0</i>	Ribosomal protein, large, P0

93

94

95

96

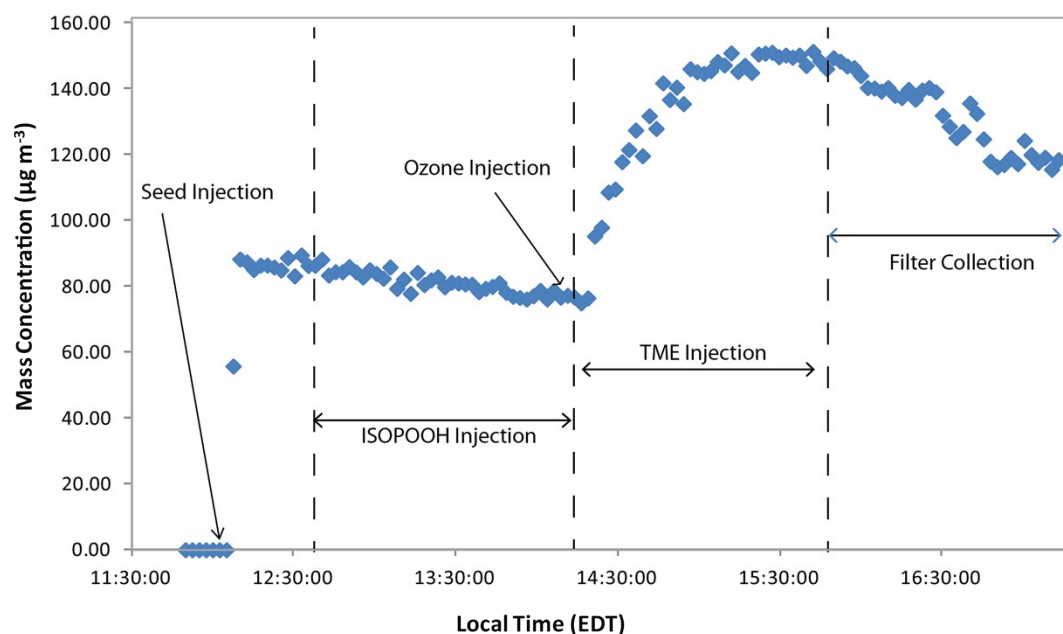
97 **Table S3.** List of genes identified with significant expression fold-changes ($p < 0.05$) upon
98 exposure to ISOPOOH-derived SOA constituents. False Discovery Rate (FDR) adjusted p-value:
99 0.05/84=0.0005.
100

Gene Symbol	Fold Regulation	p-value	NRF2-associated Genes	<FDR
<i>AKRIC2</i>	20.21	0.000003		*
<i>ALOX12</i>	1.83	0.189227		
<i>ATOX1</i>	1.57	0.000203		*
<i>BAG2</i>	2.48	0.000181		*
<i>BNIP3</i>	1.50	0.015483		
<i>DUOX2</i>	1.69	0.013911		
<i>DUSP1</i>	10.01	0.000012		*
<i>EPX</i>	2.02	0.002065		
<i>FHL2</i>	1.93	0.000212		*
<i>FTH1</i>	6.71	0.000019	+	*
<i>GCLC</i>	5.45	0.000627	+	
<i>GCLM</i>	14.12	0.000008	+	*
<i>GLA</i>	4.28	0.000019		*
<i>GPX2</i>	4.99	0.004839	+	
<i>GPX3</i>	1.88	0.002074		
<i>GSR</i>	2.66	0.002702	+	
<i>GSTP1</i>	1.70	0.000867	+	
<i>HMOX1</i>	123.64	0.00002	+	*
<i>HSP90AA1</i>	3.01	0.000014		*
<i>HSPA1A</i>	14.03	0.000441		*
<i>NCF1</i>	2.85	0.04451		
<i>NQO1</i>	6.02	0.000002	+	*
<i>PRDX1</i>	3.82	0.000009	+	*
<i>PRDX4</i>	1.56	0.009166		
<i>PRDX6</i>	2.15	0.000045		*
<i>PRNP</i>	1.85	0.000066		*
<i>PTGS1</i>	1.87	0.011846		
<i>PTGS2</i>	3.02	0.001327		
<i>RNF7</i>	1.87	0.002062		
<i>SLC7A11</i>	9.54	0.000008		*
<i>SOD1</i>	2.50	0.000203	+	*
<i>SOD2</i>	3.05	0.000002	+	*
<i>SOD3</i>	1.96	0.001269	+	
<i>SQSTM1</i>	8.67	0.00001	+	*
<i>SRXN1</i>	8.52	0.000000		*
<i>TXN</i>	3.48	0.000078	+	*
<i>TXNRD1</i>	8.71	0.001145	+	

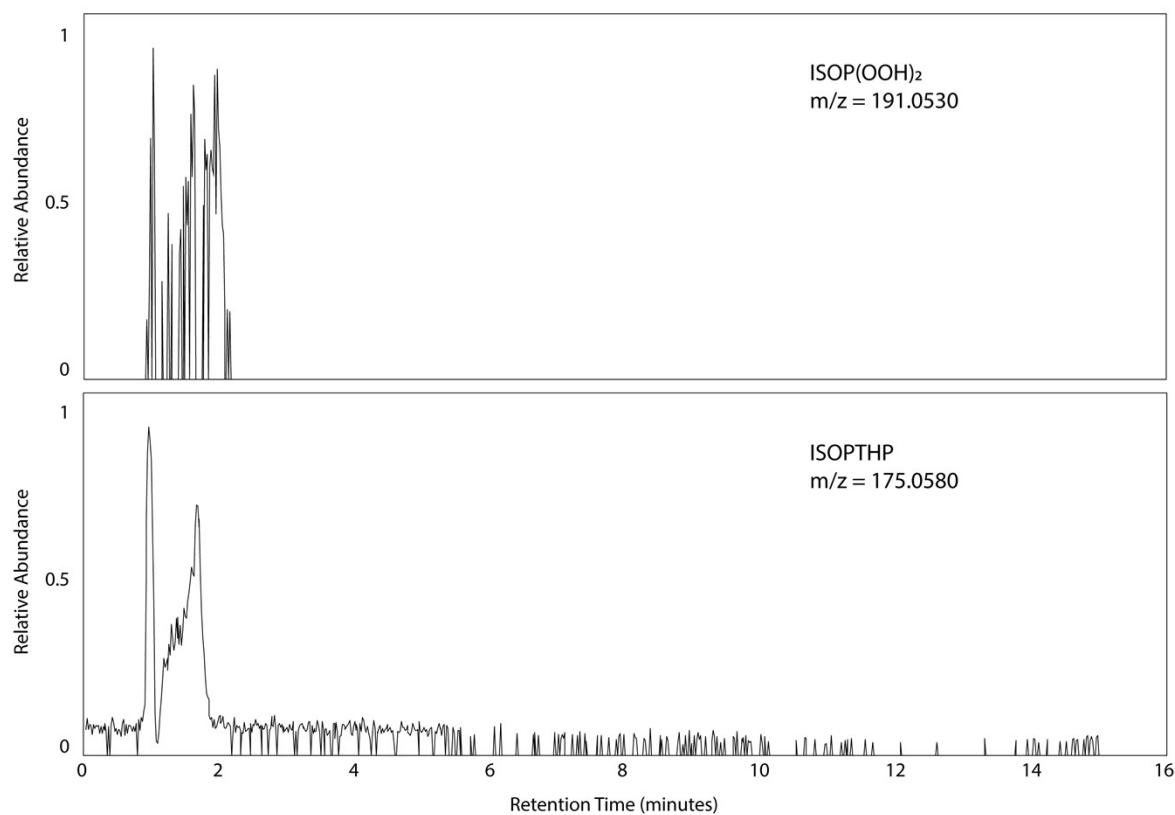
<i>UCP2</i>	2.44	0.01224		
<i>VIMP</i>	3.60	0.000002		*
<i>CAT</i>	-1.78	0.005005	+	
<i>MSRA</i>	-2.13	0.000138		*

Table S4. List of genes identified with significant expression fold-changes (p<0.05) upon exposure to ISOPOOH-derived SOA constituents. False Discovery Rate (FDR) adjusted p-value: 0.05/84=0.0005.

Gene Name	Fold Regulation	p-value	NRF2-associated Genes	<FDR
<i>AKRIC2</i>	2.20	0.013377		
<i>ATOX1</i>	1.56	0.024189		
<i>BAG2</i>	2.00	0.00763		
<i>CAT</i>	1.58	0.006833	+	
<i>DHCR24</i>	1.58	0.001557		
<i>FTH1</i>	2.28	0.008796	+	
<i>GCLC</i>	2.59	0.003719	+	
<i>GCLM</i>	2.89	0.001271	+	
<i>GLA</i>	1.74	0.034903		
<i>GPX1</i>	1.54	0.014517		
<i>GPX2</i>	5.95	0.000725	+	
<i>GPX3</i>	1.87	0.000538		
<i>GSR</i>	1.69	0.027743	+	
<i>GSTP1</i>	1.63	0.041316	+	
<i>HMOX1</i>	2.00	0.016293	+	
<i>HSP90AA1</i>	2.09	0.000988		
<i>HSPA1A</i>	1.59	0.001239		
<i>NQO1</i>	4.96	0.003367	+	
<i>PRDX1</i>	2.19	0.007017	+	
<i>PRDX3</i>	1.61	0.047334		
<i>PRDX6</i>	1.50	0.023451		
<i>PTGS1</i>	2.02	0.025923		
<i>RNF7</i>	1.78	0.040105		
<i>SIRT2</i>	1.64	0.000194		*
<i>SLC7A11</i>	3.43	0.000005		*
<i>SQSTM1</i>	2.36	0.000085	+	*
<i>SRXN1</i>	2.72	0.000015		*
<i>TXN</i>	2.23	0.016836	+	
<i>TXNRD1</i>	4.88	0.003985	+	
<i>TXNRD2</i>	1.79	0.000992		
<i>VIMP</i>	1.56	0.001192		
<i>DUOX1</i>	-2.01	0.011647		



108
 109 **Fig. S1.** Time profile of measured aerosol mass concentrations during ISOPPOOH oxidation
 110 experiments.



111
 112 **Fig. S2.** UPLC/(+)ESI-HR-QTOFMS extracted ion chromatograms (EICs) at m/z 191.0530 and
 113 175.0580 corresponding to ISOP(OOH)₂ and ISOPHP SOA constituents, respectively. Filter

114 extracts were analyzed in positive ion mode which affects sensitivity but still shows the presence
115 of hydroperoxides while not showing its large abundance.

116 **References**

- 117 1. Arashiro, M.; Lin, Y. H.; Sexton, K. G.; Zhang, Z.; Jaspers, I.; Fry, R. C.; Vizuete, W.
118 G.; Gold, A.; Surratt, J. D., In vitro exposure to isoprene-derived secondary organic aerosol by
119 direct deposition and its effects on COX-2 and IL-8 gene expression. *Atmos. Chem. Phys.* **2016**,
120 *16* (22), 14079-14090.
- 121 2. Riva, M.; Budisulistiorini, S. H.; Chen, Y.; Zhang, Z.; D'Ambro, E. L.; Zhang, X.; Gold,
122 A.; Turpin, B. J.; Thornton, J. A.; Canagaratna, M. R.; Surratt, J. D., Chemical Characterization
123 of Secondary Organic Aerosol from Oxidation of Isoprene Hydroxyhydroperoxides.
124 *Environmental Science & Technology* **2016**, *50* (18), 9889-9899.
- 125 3. Berndt, T.; Herrmann, H.; Sipilä, M.; Kulmala, M., Highly Oxidized Second-Generation
126 Products from the Gas-Phase Reaction of OH Radicals with Isoprene. *The Journal of Physical*
127 *Chemistry A* **2016**.
- 128 4. Riedel, T. P.; Lin, Y. H.; Zhang, Z.; Chu, K.; Thornton, J. A.; Vizuete, W.; Gold, A.;
129 Surratt, J. D., Constraining condensed-phase formation kinetics of secondary organic aerosol
130 components from isoprene epoxydiols. *Atmos. Chem. Phys.* **2016**, *16* (3), 1245-1254.
- 131 5. Kroll, J. H.; Ng, N. L.; Murphy, S. M.; Flagan, R. C.; Seinfeld, J. H., Secondary organic
132 aerosol formation from isoprene photooxidation. *Environmental Science & Technology* **2006**, *40*
133 (6), 1869-1877.
- 134 6. Kramer, A. J.; Rattanavaraha, W.; Zhang, Z.; Gold, A.; Surratt, J. D.; Lin, Y.-H.,
135 Assessing the oxidative potential of isoprene-derived epoxides and secondary organic aerosol.
136 *Atmospheric Environment* **2016**, *130*, 211-218.
- 137 7. Rattanavaraha, W.; Rosen, E.; Zhang, H.; Li, Q.; Pantong, K.; Kamens, R. M., The
138 reactive oxidant potential of different types of aged atmospheric particles: An outdoor chamber
139 study. *Atmospheric Environment* **2011**, *45* (23), 3848-3855.
- 140 8. Li, Q.; Wyatt, A.; Kamens, R. M., Oxidant generation and toxicity enhancement of aged-
141 diesel exhaust. *Atmospheric Environment* **2009**, *43* (5), 1037-1042.
- 142